J Clust Sci (2017) 28:3127–3138
DOI 10.1007/s10876-017-1280-3

ORIGINAL PAPER

A High-Performance Catalytic and Recyclability of Phyto-Synthesized Silver Nanoparticles Embedded in Natural Polymer

Manjari Gangarapu[1] · Saran Sarangapany[1] · Kiran Kumar Veerabhali[2] · Suja P. Devipriya[1] · Vijaya Bhaskara Rao Arava[1]

Received: 12 June 2017 / Published online: 5 August 2017

Abstract The present work deals with phytogenic synthesis of Ag NPs in the natural polymer alginate as support material using *Aglaia elaeagnoidea* leaf extract as a reducing, capping, and stabilizing agent. Ag nanoparticles embedded in alginate were characterized using UV–Vis absorption spectroscopy, Fourier transform infrared spectroscopy, field emission scanning electron microscopy, energy dispersive X-ray spectroscopy, X-ray diffraction, transmission electron microscopy techniques and selected area electron diffraction techniques. The formation of AgNPs embedded in the polymer was in spherical shape with an average size of 12 nm range has been noticed. The prepared embedded nanoparticles in polymer were evaluated as a solid heterogeneous catalyst for the reduction of 4-nitrophenol (4-NP) to 4-aminophenol (4-AP) and methylene blue to leuco methylene blue in the liquid phase using sodium borohydride ($NaBH_4$) as reducing agent. The silver nanoparticles embedded polymer exhibited extraordinary catalytic efficacy in reduction of 4-NP to 4-AP and the rate constant is 0.5054 min^{-1} at ambient conditions. The catalyst was recycled and reused up to 10 cycles without significant loss of catalytic activity. The preparation of Ag–CA composite was facile, stable, efficient, eco-friendly, easy to recycle, non-toxic, and cost effective for commercial application.

Keywords Phytogenic synthesis · *Aglaia elaeagnoidea* leaf · Ag/CA embedded nanocomposites · Catalysis

✉ Manjari Gangarapu
gangarapumanjari@gmail.com

[1] Department of Ecology and Environmental Sciences, Pondicherry University, Puducherry 605014, India

[2] Centre for Pollution Control and Environmental Engineering, Pondicherry University, Puducherry 605014, India

Introduction

Unprecedented development of nanotechnology and metal nanoparticles has triggered new and ameliorated materials for environmental remediation, catalysis, biomedical and aerospace engineering applications etc. Currently, special concern has been directed towards the Ag nanoparticles due to the highest degree of commercialization and its unique optical chemical, physical properties were differing from the bulk material and showed enhanced applications in various fields [1–3]. The potential catalytic activity of Ag nanoparticles has been implicated as an alternative technological method in the water treatment [4]. Several authors have been experimentally reported that Ag nanoparticles have potential and high catalytic and photocatalytic activities in the reduction and degradation of aromatic nitro compounds, organic pollutants, and textile dye etc., in the aqueous phase [5, 6]. However, agglomeration, stability and leaching of synthesized Ag nanoparticles, during the catalytic activity was one of the major challenges for the researchers. In this regard, surface modification of Ag nanoparticles by immobilizing/decorating on carbon, silica gel (SiO_2), metal oxides (TiO_2, ZnO, MgO etc.,), and zeolites were frequently used for the stable metal nanocatalyst by protecting nanocatalyst against aggregation and dissolution [7–9]. High stability and distribution of metal nanoparticles were not achieved by these supports due to the poor interaction between metal nanoparticles to supports such as carbon, silica etc. and thereby decreases the surface reactive sites [10]

In this framework, the search for new green synthesis for highly stable Ag nanoparticles incorporation/immobilization on a support material such as alginate, carrageenan, and chitosan etc., has been growing intriguing among the researchers [11]. The polymers/semiconductors interact and bind with the metal nanoparticles that influence the accessibility between reacting molecules and the metal nanoparticles and also alters the reaction mechanism of catalyst [12, 13]. In the production of nanoparticles as sustainable reducing and stabilizing agent by the polymers such as polyvinylpyrrolidine (PVP) [14], polyethylene glycol [15], poly (vinyl alcohol) [16], polyacrylonitrile (PAN) [17], polysaccharides [18], chitosan [19], sodium alginate [20, 21]. Large numbers of hydroxyl groups of polymers chains complex well with Ag ions and create an environment for the synthesis of Ag nanoparticles [22].

Sodium alginate (SA) natural component screened from brown marine seaweed, it is one of the main polyanionic linear polysaccharide composed of a copolymer (1,4)-linked β-D-mannuronic and (1,3) α-L-guluronic acid residues randomly arranged along the length of the chain. Based on ration and macromolecular of mannuronic and guluronic acid, alginate biocompatibility and biodegradability with metal under normal conditions were depend [23]. Alginate was used as an instant gel in the bone tissue engineering, immobilization, drug delivery, bio-sorption and also for the stabilization of metal nanoparticles due to its divalent cations adopt cross-linked chains like structure known to be “egg-box” model [24, 25]. Alginate based material was used in the cancer treatment, wound healing, antimicrobial, among biosorption capacity of alginate was well established [24]. This was used to

detach heavy metals such as chromium, cobalt, copper, nickel, and zinc etc., the capacity of sorption were in acid concentration than alkaline conditions [26]. The drawback of natural alginate gels alone is their propensity to degrade and its liquefy nature in counter ions solutions, therefore it was limited in the treatment of wastewater continuous [25]. Moreover, the metal-supported alginate gel was a perfect substrate for the effluent treatment through catalysis, because of the non-covalent interactions and electrostatic effect existence between the interactions of metal gel [27].

In this perspective, this study aimed for the synthesis of sliver nanoparticles embedded Alginate beads (Ag/CA) by using an aqueous extract of *Aglaia elaeagnoidea* leaf. This genus *Aglaia* belongs to *Meliaceae* family and is extensively distributed in coastal regions, tropical forests of Asia, Northern Australia and Pacific islands [28]. The preliminary phytochemicals screening of leaf aqueous extract of leaf exhibited the presence of steroids, phenols, flavanoids, tannins, quinones, xanthoproteins, carbohydrates and saponins which may play a crucial role in tuning and stabilizing of metal nanoparticles [29]. Henceforth, we focus on the application of green chemistry principles for the synthesis of Ag nanoparticles embedded in the natural origin support material alginate, an eco-friendly approach and evaluated their efficacy for the catalytic reduction of pernicious organic pollutant 4-nitrophenol (4-NP) to 4-aminophenol (4-AP) from aqueous phases by heterogeneous method were demonstrated. To the best of our knowledge, *A. elaeagnoidea* leaf extract derived Ag/CA nanocomposite and its catalytic role for the 4-NP and MB reduction were evaluated for the first time.

Experimental Section

Materials

Silver nitrate ($AgNO_3$), and Calcium chloride ($CaCl_2$) were purchased from Merck, sodium alginate, 4-nitrophenol and Sodium borohydride (4-NP), was purchased from Sigma–Aldrich. The *A. elaeagnoidea* leaves were collected from Pondicherry University, India and dried and ground to fine powder. About 10 g of leaf powder and 125 ml of distilled water were taken in conical flask refluxed for 15 min on a magnetic stirrer. The extract has filtered by Whatman Filter paper to separate fine plant debris and stored at in 4 °C for further experiment.

Preparation of Silver Embedded Alginate (Ag/CA) Beads Using Phyto-Synthesis Method

Sodium alginate (1%, w/v) mixed with 100 ml of 1 M $AgNO_3$ solution and dissolve completely by stirring with sonication for 10 min, 10 ml of leaf extracts of *A. elaeagnoidea* were added and stirred the mixture continuously for 20 min at the room temperature. The Ag/alginate/extract mixture was taken in the burette, added drop by drop into 150 ml of 0.1 M $CaCl_2$ under magnetic stirrer light brown color solution to golden yellow beads in the $CaCl_2$ solution were formed. These beads was

kept in the $CaCl_2$ solution for 2 h for diffusion of Ca_2 ions and washed with deionized water several times to detach excess of chlorine. Finally, CA (calcium beads) beads were kept in the distilled water used for the further [30].

Instruments

The cryo-ground Ag/CA nanocomposite and CA hydro beads samples were used for characterization studies. UV–Vis absorption spectrum were recorded in a UV–VIS–NIR Spectrophotometer (Make: Varian Model: 5000) at ambient conditions. Transmission electron microscopy (TEM) images with SAED (Selected area electron diffraction) were obtained in a JEOL model 2010, at an accelerating voltage of 200 keV along with wavelength (k) of 0.0251 Å. The samples were prepared by suspension of cryo ground Ag/CA beads in ethanol were prepared for the line-scan profiles and elemental mapping through energy-dispersive x-ray spectroscopy (Scanning Electron Microscope along with EDAX, S3700N). X-ray diffraction pattern (XRD) analysis was carried out using a Cu-Ká radiation by a diffractometer (Philips PW 3710/3020). FTIR spectra were obtained on Thermo Nicolet; model 6700 with KBr method. The loading and leaching of Ag/CA nanocomposite after catalytic application were determined by a Inductively Coupled Plasma-Atomic Emission Spectrometer (ICPAES, Model: JobinYvon Horiba).

Catalysis Studies

The catalytic activity of Ag embedded CA nanocomposite was performed in 3 ml quartz with 144.8 mg of Ag/CA as an optimal dosage for the reduction of 1 ml of 10^{-3} M 4-NP with 1 ml of 10^{-2} M sodium borohydride ($NaBH_4$) as a model reaction. The quartz was immediately inserted in the UV–Vis spectrophotometer and recorded the catalytic reduction rate at different time intervals, between 200 and 600 nm at the room temperature. Reduction of yellow color to colorless indicates the formation of 4-AP. The same dose of catalyst was used for the reduction of 1 ml 10^{-4} MB in the presence of $NaBH_4$ reducing agent, change of color were observed in few seconds and UV–Vis spectrophotometer declined to record in few seconds.

Recyclability, and Stability

The dosage of catalyst were studied from the range of 5 mg to 2 g and 144.8 mg was taken as an optimal dosage for the reduction of 1 ml of 10^{-3} M 4-NP and 10^{-4} MB with 1 ml of 10^{-2} M sodium borohydride. The 4-NP reduction and formation of the 4-AP process were investigated by the UV–Vis spectrophotometer, the catalyst was the recovery by simple filtration and reused in next successive cycles after rinsing in the distilled water.

Results and Discussion

Mechanism Involved in the Formation of Ag NPs

The formation of embedded Ag nanoparticles using *A. elaeagnoidea* leaf extract confirmed by its color change visibly and its possible mechanism was based on phytochemicals presence in the extract such as total phenols, steroids, flavonoids, tannins, Coumarins, Quinones, Xanthoproteins, Carbohydrates and saponins etc. [31]. These are plays a crucial role in the formation of embedded Ag nanoparticles. The possible involvement of phytochemicals in the synthesis of Ag nanoparticles was explained (Scheme.1). The total phenols are mainly utilized in the reduction of Ag^{+} ions and other phytochemical constituents acts binding agent for embedded Ag nanoparticles, while all these bio-compounds are being oxidized to ketonic structures with the metal ions and reduced readily in the reduction reaction matrix [32].

UV–Vis Spectroscopy

The formation Ag embedded alginate beads were observed visibly by change in color white color to gold yellow (Fig. 1a, b). The formation of optical spectra of embedded Ag NPs in CA gel beads was confirmed using the UV–Vis spectroscopy. Figure 2 showed the surface plasmon resonance absorbance at 430 nm region confirms the formation of Ag NPs in hydro gel [30].There is no optical absorption peak was observed for the polymer alone in the UV–VIS spectrophotometer [33].

Morphological Features

Morphological and average size of Ag nanoparticles embedded in alginate was analyzed by TEM. The spherical shaped Ag nanoparticles were embedded in CA

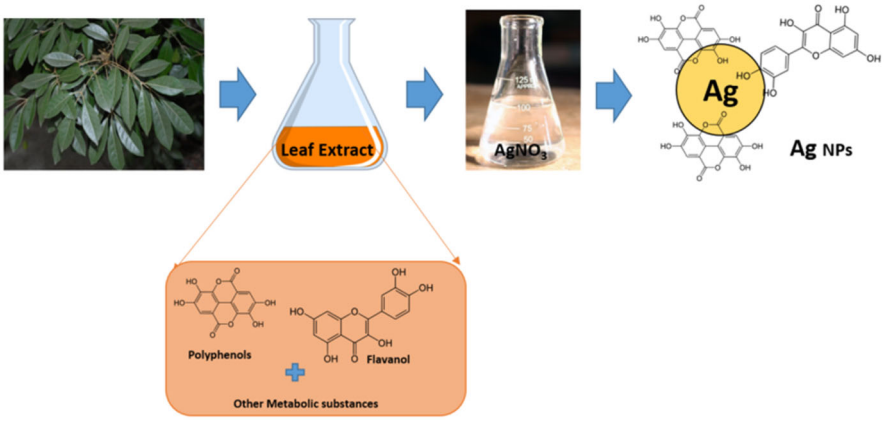

Scheme 1 Possible phytochemical constituents mechanism involved in the synthesis of Ag NPs

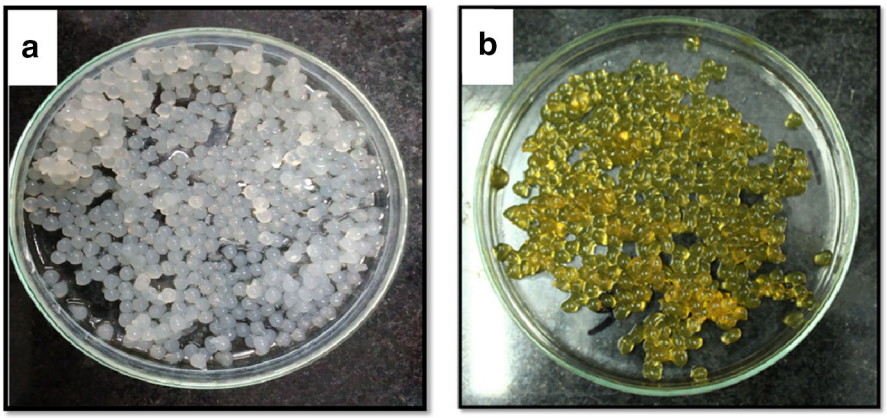

Fig. 1 Image of **a** pure alginate beads **b** Ag/CA beads

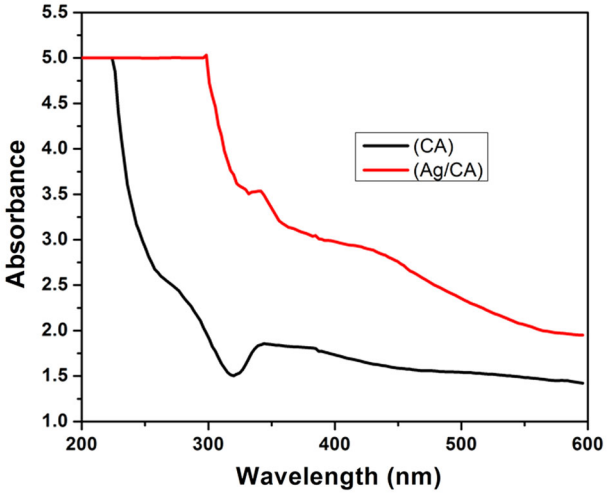

Fig. 2 UV–Visible spectra of pure and Ag/CA

with an average size of 7–12 nm (Fig. 3a, b respectively). The SAED patterns for the obtained Ag nanoparticles were shown the Fig. 3c, indicates clearly the crystalline nature of formed nanoparticles. Figure 4 shown EDAX graph, revealed the presence of the elemental silver, and calcium, indicating the reduction of elemental silver into silver nanoparticles embedded in the calcium alginate.

Crystallographic Nature

XRD spectral patterns of Ag/CA were shown in Fig. 5 (JCPDS file No.004-0783) which confirms the single-phase crystalline Ag NPs embedded in alginate hydro beads. A number of Bragg reflections for face-centered cubic (fcc) metallic silver, at

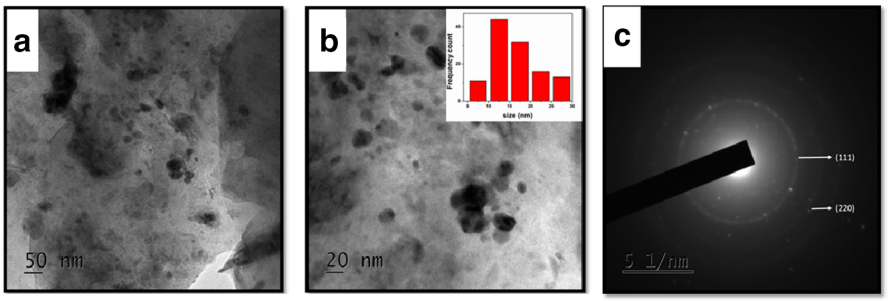

Fig. 3 **a**, **b** TEM image of Ag/CA (*Inset* particle size distribution). **c** SAED pattern of Ag/CA beads

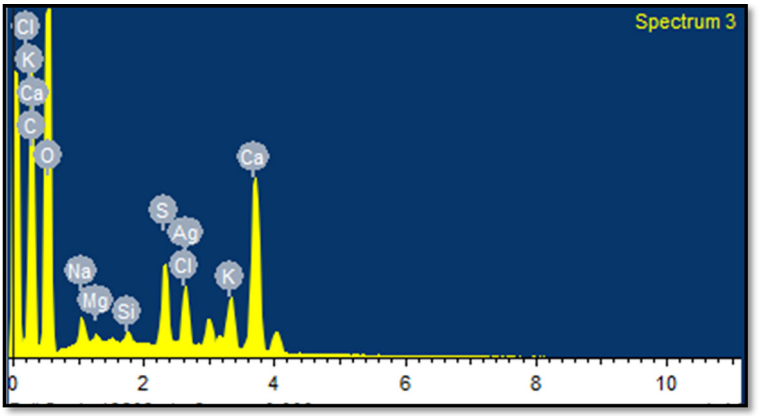

Fig. 4 EDAX graphof Ag/CA

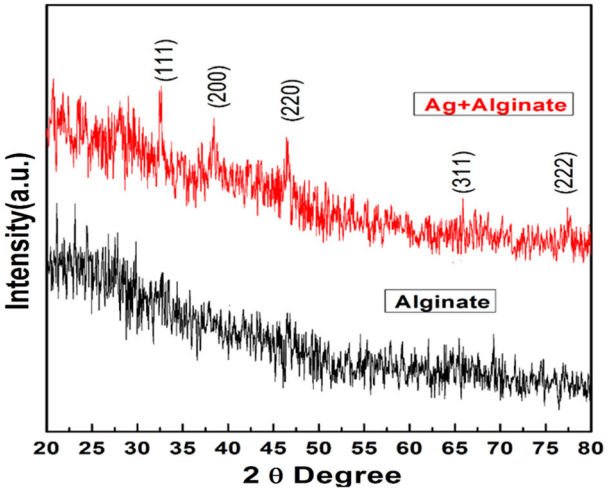

Fig. 5 XRD of cryo grind pure and Ag/CA

$2\theta = 32.63$, 38.26, 46.57, 64.80, and 77.84 corresponding to (111), (200), (220), (311) and (222) planes respectively [34]. The Ag/CA, average crystalline size were calculated from full width half maximum of Bragg reflections using Debye–Scherrer equation [35].

$$D = \frac{0.9/\lambda}{\beta \cos \theta} \quad (1)$$

where "λ" is X-ray wavelength i.e., 0.1541 nm, "β" is the full width half maximum in radians, and "θ" is the Bragg's angle. Based on the different 2θ peaks of Ag/CA, we calculated an average crystalline size ca. 7.1 nm Ag nanoparticles embedded in alginate.

FTIR Analysis

The probable phytochemicals of *A. elaeagnoidea* leaf extract responsible for the synthesis and stabilization of Ag nanoparticles in CA beads could be achieved using FTIR analysis. Figure 6 showed the FTIR spectrum of leaf extract and cryo-grinded AgNPs embedded CA beads show. The prominent peaks of leaf extract exhibited at 3434, 2921, 2723, 1633, 1456, 1025, and 900–449 cm^{-1} respectively, which corresponding to the alcoholic/carboxylic O–H group of phenolic compounds, =C–H aldehydic stretch of primary and secondary amines along with amide linkage of proteins, C–H alkenes bending of ketones and esters and Alkyl Halide group compounds were present. The intensity of all the bands was almost reduced in the cryo-grinded Ag/CA beads, the reduced and shifting intensity in FTIR band spectra indicated the involvement of phytochemicals in the formation of Ag nanoparticles in the polymer [36, 37].

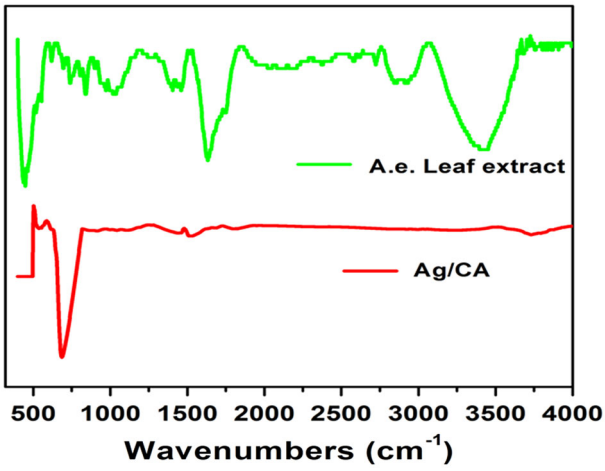

Fig. 6 FTIR spectrum of *A. elaeagnoidea* leaf extract and Ag/CA beads

Catalytic Activity

In the catalytic activity of particles, surface area plays a crucial role while a change in the morphological features and size will definitely affect the catalyst specific surface area [38]. The spherical shaped NPs with high specific surface area embedded polymer thus act as promising active and stable catalyst. Therefore, we selected the conversion of 4-NP to 4-AP and MB to leuco methylene blue (LMB) as a model reaction for evaluating the catalytic efficiency of AgNPs/CA hydro gels. The electron transfer from $NaBH_4$ to MB dye in the presence of Ag/CA catalyst and absorbed on a surface of the catalyst via π-π stacking interactions, thereby reduction of dye to LMB. The maximum UV–Visible absorption band of MB dye at 664 nm with a shoulder at 614 nm [29]. The reduction reaction of 4-NP and MB using $NaBH_4$, in the presence of Ag/CA catalyst were monitored using UV–Vis spectrophotometer. Complete reduction of MB dye within few seconds (45 s) were observed from the Fig. 7. Theoretically, the reduction reaction of 4-NP completed in two reaction steps. In the first, by adding a reducing agent ($NaBH_4$) into liquid phase 4-NP, the solution color changed from pale to dark yellow by the converting 4-nitrophenol as 4-nitrophenolate ions. The formation of 4-nitrophenolate ions was due to alkaline condition of $NaBH_4$ and the characteristic red shift in the absorption peak from 317 nm to 400 nm were observed (Fig. 8a). Conversely, after the addition of Ag/CA catalyst contained Ag nanoparticles, the UV–Vis absorption peak intensity were decreased gradually from 400 nm to 300 nm with increase in the reaction time (Fig. 8a). The absorption peak at 300 nm indicates the formation of 4-AP [39]. The initial concentration of reducing agent exceeds, the rate of reduction could be assumed as independent of BH_4. Hence, to assess the catalytic reaction rate it follows kinetics pseudo-first-order regards to the 4-NP concentration might be used. The absorbance of 4-NP at a time A_t to A_o measured at $t = 0$, equal

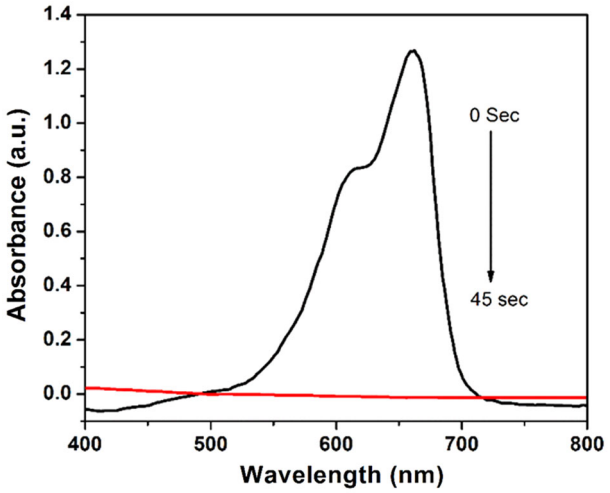

Fig. 7 Reduction of MB to LMB by Ag/CA

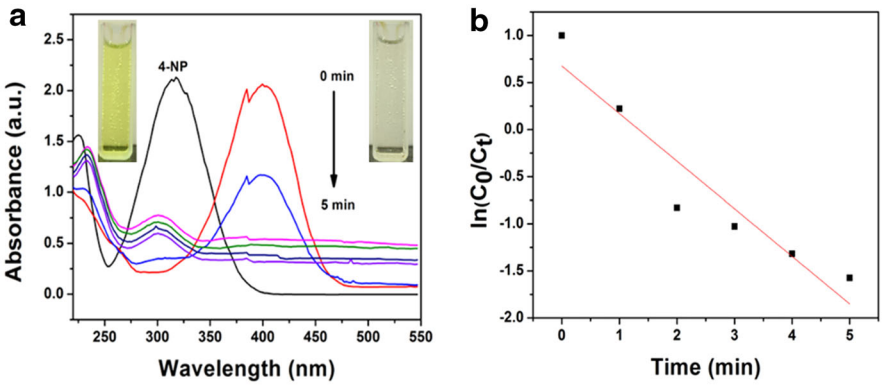

Fig. 8 Reduction of 4-NP to 4-AP by Ag/CA. **a** Heterogeneous catalysis and **b** rate constant

to C_t/C_o of 4-NP concentration ratio. The kinetics reaction equation could be described as [40]:

$$-\mathrm{In}(C_t/C_0) = \mathrm{In}(A_t/A_0) = k_t \quad (2)$$

where 'k' is the rate constant for the catalyst at known time and A_t/A_0, the absorbance of solution mixture at the reaction time. C_0 and C_t, 4-NP concentrations.

A good linear relation among $\mathrm{In}(A_t/A_0)$ and the reaction rate constant (k) might be calculated by slope of linear sections of plot (Fig. 8b) and about more than 80% of conversion at the reaction rate constant of Ag NPs (0.5054 min^{-1}). Table 1 illustrates the comparison of catalyst efficiency of embedded Ag nanoparticles with the previously reported literature metal nanoparticles support on different material.

Recyclability and Stability

For the practical application of Ag/CA beads, its stability and recyclability was most important. The stability of Ag NPs embedded polymer was evaluated for the formation of 4-AP using 4-NP and reduction MB to LMB for 10 consecutive cycles. The reactions were monitored using UV–Vis spectrum and are capable of

Table 1 Comparison of 4-NP reduction

S. no.	Material	Time	References
1	Au/microgel nanocomposite	2.44×10^{-2} s^{-1}	[40]
2	Ag NPs/PD/PANFP composite	0.1370 min^{-1}	[41]
3	Ag@HTO-PDA	3.14×10^{-3} s^{-1}	[42]
4	MBS-AuNPs Starch	0.0218 min^{-1}	[43]
5	CTAB/Ag nanohybrid	1.2×10^{-3} s^{-1}	[44]
4	AgNPs/MWCNTs-chiston composite	0.473 min^{-1}	[45]
7	Ag/CA beads	0.5054 min^{-1}	Present work

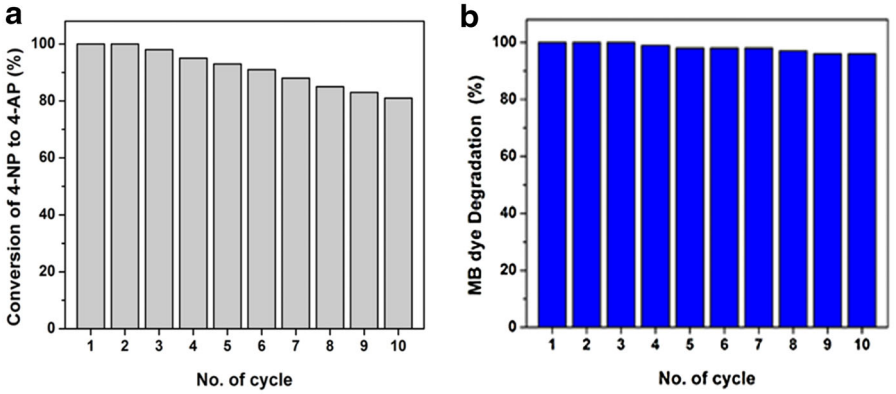

Fig. 9 Recyclability and reuse of Ag/CA beads for reduction of **a** 4-NP, **b** MB

conserving above 80% after 10 cycles (Fig. 9a, b). The Ag/CA beads were recovered by simple filtration and reused after washing in distilled water. The leaching of Ag NPs from the beads after catalytic reactions were was tested by ICPAES, no significant loss of catalyst was observed (<4%).

Conclusion

A novel and facile recyclable Ag/CA catalyst was synthesized using *A. elaeagnoidea* leaf extract for the formation of 4-AP compounds. The green synthesized nanocomposite formation was confirmed by its characterization results, using UV–Vis spectra, FTIR, SEM, EDX, XRD, TEM and SAED. Spherical Ag nanoparticles with 7–12 nm size were embedded in CA. The minimal optimal dose of green synthesized catalyst used for the catalytic reduction of 4-NP and MB at room temperature. Eminently high catalytic activity performance with excellent stability up to 10 cycles with more than 80% of conversion was obtained. There is no significant leaching of Ag content in Ag/CA nanocomposites, confirmed with ICPAES results. Therefore, low cost green synthesized Ag embedded CA nanocomposite with high catalytic performance could be used for the large scale synthesis of nanocomposite and open a green route for commercial applications in future.

Acknowledgements The authors are thankful to Pondicherry University for providing fellowship. The authors are acknowledge central instrumentation facility, Pondicherry University for characterization analysis. We also thanks to Ms. Savitha Veeraragavan for their continuous encouragement during the work.

References

1. J. Pulit-Prociak and M. Banach (2016). *Open Chem.* **14**, 91.
2. A. Moisala, A. G. Nasibulin, and E. I. Kauppinen (2003). *J. Phys. Condens. Matter.* **15**, 3011.

3. H. Barabadi, S. Honary, M. A. Mohammadi, E. Ahmadpour, M. T. Rahimi, A. Alizadeh, F. Naghibi, and M. Saravanan (2017). *Environ. Sci. Pollut. Res.* **24**, 5810.
4. A. Bée, D. Talbot, S. Abramson, and V. Dupuis (2011). *J. Colloid Interface Sci.* **362**, 492.
5. T. B. Devi and M. Ahmaruzzaman (2016). *Environ. Sci. Pollut. Res.* **23**, 17714.
6. H. Huang and X. Yang (2004). *Carbohydr. Res.* **339**, 2631.
7. P. Zhang, C. Shao, Z. Zhang, M. Zhang, J. Mu, Z. Guo, and Y. Liu (2011). *Nanoscale* **3**, 3363.
8. S. N. Hosseini, S. M. Borghei, M. Vossoughi, and N. Taghavinia (2007). *Appl. Catal. B* **74**, 62.
9. A. Hatamifard, M. Nasrollahzadeh, and S. M. Sajadi (2016). *New J. Chem.* **40**, 2513.
10. L. Ai, H. Yue, and J. Jiang (2012). *J. Mater. Chem.* **22**, 23453.
11. E. Ruiz-Hitzky, K. Arigaand Y. M. Lvov (eds.), (Wiley, 2008).
12. L. N. Lewis (1993). *Chem. Rev.* **93**, 2730.
13. D. Chunfa, Z. Xianglin, C. Hao, and C. Chuanliang (2016). *Rare Metal Mater. Eng.* **45**, 266.
14. W. J. Jin, H. K. Lee, E. H. Jeong, W. H. Park, and J. H. Youk (2005). *Macromol. Rapid Commun.* **26**, 1907.
15. C. Luo, Y. Zhang, X. Zeng, Y. Zeng, and Y. Wang (2005). *J. Colloids Interface Sci.* **288**, 448.
16. S. Chaudhari, Y. Kwon, M. Moon, M. Shon, S. Nam, and Y. Park (2016). *Bull. Korean Chem. Soc.* **37**, 1991.
17. Y. Liu, G. Jiang, L. Li, H. Chen, Q. Huang, T. Jiang, and X. Du (2016). *MRS Commun.* **6**, 40.
18. H. E. Emam and H. B. Ahmed (2016). *Carbohydr. Polym.* **135**, 307.
19. E. M. Azzam, S. M. Solyman, and A. A. Abd-Elaal (2016). *Colloids Surf.* **A510**, 230.
20. M. Faried, K. Shameli, M. Miyake, A. Hajalilou, A. Zamanian, Z. Zakaria, E. Abouzari-lotf, H. Hara, N. B. Ahmad Khairudin, and M. F. Binti Mad Nordin (2016). *J. Nanomater.* 11.
21. Q. Wang, S. Liu, H. Wang, and Y. Yang (2016). *Phys. Chem. Chem. Phys.* **18**, 12615.
22. K. Varaprasad, G. M. Raghavendra, T. Jayaramudu, and J. Seo (2016). *Carbohydr. Polym.* **135**, 355.
23. L. V. Trandafilović, D. K. Božanić, S. Dimitrijević-Branković, A. S. Luyt, and V. Djoković (2012). *Carbohydr. Polym.* **88**, 269.
24. T. A. Davis, B. Volesky, and A. Mucci (2003). *Water Res.* **37**, 4330.
25. E. Torres, Y. N. Mata, M. L. Blazquez, J. A. Munoz, F. Gonzalez, and A. Ballester (2005). *Langmuir* **21**, 7958.
26. D. Kratochvil and B. Volesky (1998). *Trends Biotechnol.* **16**, 300.
27. V. K. Gupta, M. L. Yola, T. Eren, F. Kartal, M. O. Çağlayan, and N. Atar (2014). *J. Mol. Liq.* **190**, 138.
28. K. K. N. Nair (1981). Bombay Nat. *Hist. Soc. J.* **78**, 432.
29. G. Manjari, S. Saran, T. Arun, A. V. Rao, and S. P. Devipriya (2017). *J. Saudi Chem. Soc.*. doi:10.1016/j.jscs.2017.02.004a.
30. S. Saha, A. Pal, S. Kundu, S. Basu, and T. Pal (2009). *Langmuir* **26**, 2893.
31. G. Manjari, S. Saran, A. V. Rao, and S. P. Devipriya (2017). *I. J. Ayurveda Pharma. Res.* **5**, 6.
32. K. Anand, K. Kaviyarasu, S. Muniyasamy, S. M. Roopan, R. M. Gengan, and A. Chuturgoon (2017). *J. Clus. Sci.* **28**, 2291.
33. A. Pal, K. Esumiand, and T. Pal (2005). *J. Colloid Interface Sci.* **288**, 401.
34. S. Waghmode, P. Chavan, V. Kalyankar, and S. Dagade (2013). *J. Chem.* **2013**, 5.
35. H. Borchert, E. V. Shevchenko, A. Robert, I. Mekis, A. Kornowski, G. Grübel, and H. Weller (2005). *Langmuir* **21**, 1936.
36. C. T. Kamala, K. H. Chu, N. S. Chary, P. K. Pandey, S. L. Ramesh, A. R. Sastry, and K. C. Sekhar (2005). *Water Res.* **39**, 2826.
37. P. Velmurugan, M. Cho, S. M. Lee, J. H. Park, K. J. Lee, H. Myung, and B. T. Oh (2016). *J. Saudi Chem. Soc.* **20**, 320.
38. B. Roldan Cuenya (2012). *Acc. Chem. Res.* **46**, 1691.
39. G. Manjari, S. Saran, T. Arun, S. P. Devipriya, and A. V. Rao (2017). *J. Clus. Sci.* **28**, 2056.
40. N. P. B. Tan, and C. H. Lee (2017). *Green Chem. Process. Synthesis*.
41. S. Lu, J. Yu, Y. Cheng, Q. Wang, A. Barras, W. Xu, S. Szunerits, D. Cornu, and R. Boukherroub (2017). *Appl. Surf. Sci.* **411**, 169.
42. E. Cao, W. Duan, F. Wang, A. Wang, and Y. Zheng (2017). *Carbohydr. Polym* **158**, 50.
43. S. Chairam, W. Konkamdee, and R. Parakhun, (2015). *J. Saudi. Chem. Soc.*
44. X. An, Y. Long, and Y. Ni (2017). *Carbohydr. Polym* **156**, 258.
45. S. M. Alshehri, T. Almuqati, N. Almuqati, E. Al-Farraj, N. Alhokbany, and T. Ahamad (2016). *Carbohydr. Polym* **151**, 143.